Conical Refraction of a high-M^2 laser beam

G. S. Sokolovskii[a], V. Yu. Mylnikov[b], S. N. Losev[a], K. A. Fedorova[c,d], E. U. Rafailov[c,d]

[a]Ioffe Institute, St. Petersburg, Russia
[b]Peter the Great St. Petersburg Polytechnic University, St. Petersburg, Russia
[c]School of Engineering and Applied Science, Aston University, Birmingham, UK
[d]ITMO University, St. Petersburg, Russia

ABSTRACT

We report on experiments with conical refraction of laser beams possessing a high beam propagation parameter M^2. With beam propagation parameter values M^2=3 and M^2=5, unusual Lloyd's distributions with correspondingly three and five dark rings were observed. In order to explain this phenomenon, we extend the dual-cone model of the conical refraction that describes it as a product of interference of two cones that converge and diverge behind the exit facet of the crystal. In the extended model, these converging/diverging cones are represented as the cone-shaped quasi-Gaussian beams possessing the M^2 parameter of an original beam. In this formalism, a beam-waist of these cone-shaped beams is proportional to the M^2 value and defines the area of their interference which is a width of the Lloyd's ring. Therefore, the number of dark rings in the Lloyd distribution is defined by the M^2 value and can be much greater than unity. The results of the numerical simulations within the extended dual-cone model are in excellent agreement with the experiment.

Keywords: Birefringence, crystal optics; geometric optics; laser diodes, conical refraction, Gaussian beams

1. INTRODUCTION

Conical refraction (CR) is a phenomenon with almost 200 years of research history[1-3]. It is observed when a narrow beam of light propagates along one of the optical axes of a biaxial crystal. Such a beam evolves as a hollow double-walled cylinder of light behind the exit facet of a crystal. The typical evolution of the CR profile is shown in Fig.1. At the focal plane (also known as the Lloyd's plane)[2], two asymmetrical bright rings are visible. The radius of the separating dark ring is given by a simple relation: $R_0 = L\chi$, where L is a crystal length and 'conicity' is given by $\chi = \sqrt{(n_2 - n_1)(n_3 - n_2)}/n_2$, with n$_1$, n$_2$ and n$_3$ being refractive indexes (n$_1$<n$_2$<n$_3$). This separating dark ring (termed as the Poggendorf's ring)[3] is the most clearly visible before and after the Lloyd's plane. Another important feature of conical refraction (known as Raman spots)[4] concluding the axial evolution of CR pattern was observed more than a century after the first CR experiments.

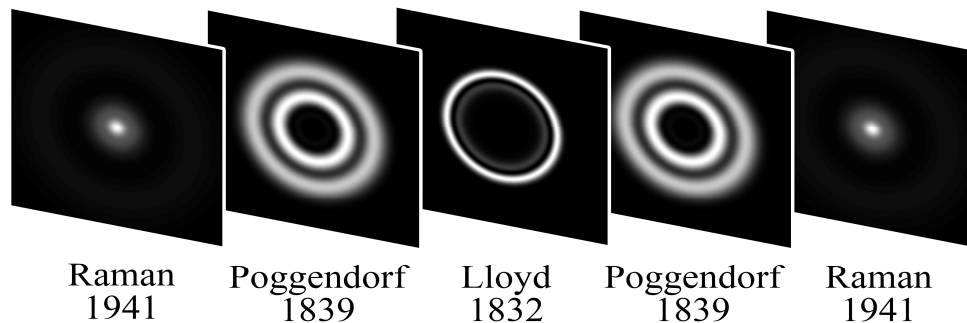| Raman	Poggendorf	Lloyd	Poggendorf	Raman
1941	1839	1832	1839	1941

Figure 1. The evolution of the CR beam profile.

Although the practical applications of CR has been limited by the difficulties associated with cutting of the biaxial crystals with the necessary precision, a few recent papers report on ultra-efficient CR lasers[5,6], lasers with CR output from the plane mirror[7], optical trapping with CR beams[8], utilization of CR for quantum computing and cryptography[9] and super-resolution microscopy[10]. All these applications attracted our attention to the research of CR of the beams of semiconductor lasers, which are the most compact and efficient sources of radiation but often feature the high value of the beam propagation parameter M^2.

2. THEORY

2.1 Background theory and a dual-cone model

The exact theoretical model of CR phenomenon was first developed by A.M. Belsky and A.P. Khapalyuk[11] and more recently by M.V. Berry[12]. According to this model the unpolarized light passing through a CR crystal can be represented as the electric displacement vector $\mathbf{D}$ expressed in the form: $\mathbf{D} = [B_0 + B_1]\left(\begin{smallmatrix} d_x \\ d_y \end{smallmatrix}\right)$ with B_l described as:

$$B_l(R,Z) = k\int_0^\infty Pa(P)\exp(-\frac{1}{2}ikZP^2)\cos(kR_0P - l\frac{\pi}{2})J_l(kRP)dP \tag{1}$$

where $l=0,1$ is the integer number, k is the crystal wavenumber, kP is the transverse wavevector (with $P \ll 1$ due to paraxiality), R_0 is the radius of conical refraction beyond the crystal, Z is the normalized distance, J_l is the Bessel function of the first kind of order l, and $a(P)$ is the Fourier transform of the incident beam profile. For the Gaussian beam $G_0(R) = \exp(R^2/2w^2)$ the Fourier transform is $a(P) = kw^2\exp(-k^2w^2P^2/2)$. The light intensity is then: $I = \mathbf{D}\cdot\mathbf{D}^*$, which, in the case of unpolarized light because of absence of the interference between B_0 and B_1[12], can be simplified to $I = |B_0 + B_1|^2 = |B_0|^2 + |B_1|^2$

Using the normalized variables expressed as:

$$r = \frac{R}{R_0}, \quad z = \frac{Z}{kwR_0}, \quad \rho = \frac{R_0}{w}, \quad s = kwP \tag{2}$$

formula (1) takes the following form:

$$B_l(r,z) = \int_0^\infty s\exp(-\frac{1}{2}(1+i\rho z)s^2)\cos(\rho s - l\frac{\pi}{2})J_l(r\rho s)ds \tag{3}$$

Also, G.S.Sokolovskii et al.[13] and later on A.Turpin et al.[14] have shown that these equations can be transformed in a way enabling the electric displacement vector $\mathbf{D}$ to be written as: $\mathbf{D} = [C_1 + C_2]\left(\begin{smallmatrix} d_x \\ d_y \end{smallmatrix}\right)$ with functions $C_{1,2}$ given by:

$$C_{1,2}(r,z) = \int_0^\infty s\exp(-\frac{1}{2}(1+i\rho z)s^2 \pm i\rho s)[J_0(r\rho s) \mp i\cdot J_1(r\rho s)]ds \tag{4}$$

In this expression C_1 and C_2 are the two cones, converging and diverging behind the exit plane of the CR crystal, and intersecting in the Lloyd's plane. For the case $\rho \gg 1$ we can use asymptotic approximations for Bessel functions. Noting $r \geq 0$, integration of (4) yields:

$$C_{1,2}(r>0,z) = \frac{1}{\sqrt{8r\rho}}\frac{1}{(1+i\rho z)^{3/4}}\exp(-\frac{\rho^2(r-1)^2}{4(1+i\rho z)} \pm i\pi/4)D_{-1.5}(\pm\frac{i\rho(r-1)}{\sqrt{1+i\rho z}}) \tag{5}$$

where D_l is the Parabolic cylinder function of order l. Hereafter we shall consider only the converging cone C_1 taking into account the conical refraction is symmetrical about z axis.

2.2 Lloyd's plane and transitional region

Let us expand D_l in series in the vicinity of $r=1$ in the Lloyd's plane $z=0$. This enables approximation of the squared absolute value of (5) by Gaussian distribution of a width $w_1 = m^2w$, where $m^2 = \sqrt{2}\Gamma(3/4)\left[3\cdot\Gamma(3/4)^2 - 4\cdot\Gamma(5/4)^2\right]^{-1/2} \approx \pi/2$. This yields:

$$I_1(r>0,0) = |C_1(r>0,0)|^2 = \frac{A^2}{\rho r}\exp\left(-\frac{\rho^2(r-1)^2}{m^4}\right)$$ (6)

with $A = \sqrt{\pi}\,2^{-9/4}\Gamma^{-1}(5/4)$.

Now we consider the area of $r>0$ and $z>0$ where the cone approaches z axis. Assuming $z \gg 1/\rho$, we can simplify the argument of the parabolic cylinder function in (5). Again, expanding this in series in the vicinity of r_{max} and approximating it by the Gaussian function of $r_{max} = 1 - z/\sqrt{2}$ we get

$$I_1(r>0,z>0) = \frac{1}{\rho r}\frac{B^2}{\rho z}\exp\left(-\frac{(r-(1-z/\sqrt{2}))^2}{z^2/2}\right)$$ (7)

where $B = 2^{3/4}e^{-1/4}\pi^{-1/2}$.

2.3 Conical quasi-Gaussian beams

Noticing similarity between (6) and (7) we define the dimensionless width of the conical beam similar to the classical Gaussian beam[15]:

$$\sigma(z) = m^2\sqrt{1+\frac{\rho^2 z^2}{2m^4}}$$ (8)

which gives:

$$I_1(r>0,z) = \frac{A^2}{\rho r}\frac{1}{\sqrt{1+\rho^2 z^2/2m^4}}\exp\left(-\frac{\rho^2(r-(1-z/\sqrt{2}))^2}{m^4(1+\rho^2 z^2/2m^4)}\right)$$ (9)

Due to the aforementioned approximations, the amplitude factor in the transitional region (7) does not differ substantially from the amplitude factor of expression (9). In this respect, we make the energy conservation correction of this approximate solution, sticking to its simple form, and shall use expression (9) hereafter. Formula (9) demonstrates that CR can be described as a superposition of conical quasi-Gaussian beams. In general case, similarly to an oblique Gaussian beam, one can describe a conical quasi-Gaussian beam as:

$$E(R,Z) = \frac{w}{R}\frac{A_0}{(1+\tilde{Z}(R,Z)^2/Z_0^2)^{1/4}}\exp\left(-\frac{\tilde{R}(R,Z)^2}{2W^2(1+i\cdot\tilde{Z}(R,Z)/Z_0)}+ik\tilde{Z}(R,Z)+i\beta\right)$$ (10)

where $\tilde{R} = (R-R_0)\cdot\cos(\alpha)-Z\cdot\sin(\alpha)$, $\tilde{Z} = (R-R_0)\cdot\sin(\alpha)+Z\cdot\cos(\alpha)$, α is a beam inclination angle relatively to z axis. Using the paraxial approximation we can write $\sin(\alpha)\approx\alpha$, $\cos(\alpha)\approx 1$ and $\tilde{R} = (R-R_0)-Z\cdot\alpha$, $\tilde{Z} = (R-R_0)\cdot\alpha+Z$. Then the expression (10) can be rewritten in the following way:

$$E(R,Z) = \frac{w}{R}\frac{A_0}{(1+Z^2/Z_0^2)^{1/4}}\exp\left(-\frac{((R-R_0)-Z\cdot\alpha)^2}{2W^2(1-i\cdot Z/Z_0)}+ikZ+ik(R-R_0)\cdot\alpha+i\beta\right)$$ (11)

Using (11), (9) and (5), we finally get: $A_0 = A$, $W = w\cdot m^2$, $Z_0 = \sqrt{2}m^2 k\cdot w^2 = \sqrt{2}k\cdot W^2$, $\alpha = \mp\dfrac{1}{\sqrt{2}kw}$, $\beta = \pm\dfrac{\pi}{4}$ for C_1 and C_2 respectively, which gives:

$$C_{1,2}(r>0,z) = \frac{A}{\sqrt{\rho r}}\frac{1}{(1+\rho^2 z^2/2m^4)^{1/4}}\exp\left(-\frac{\rho^2(r-(1\mp z/\sqrt{2}))^2}{2m^4(1-i\,\rho z/\sqrt{2}m^2)}\mp i\left(\frac{\rho(r-1)}{\sqrt{2}}-\frac{\pi}{4}\right)\right)$$ (12)

In this way, the intensity of conically refracted radiation $I = |C_1+C_2|^2$ in the Lloyd's plane $z=0$ takes the form:

$$I(R,0) = \frac{4A^2 w}{R} \exp\left(-\frac{(R-R_0)^2}{m^2 w^2}\right) \cos^2\left(\frac{(R-R_0)}{w\sqrt{2}} - \frac{\pi}{4}\right) \tag{13}$$

Expression (13) clearly shows that the dual-ring distribution in the Lloyd's plane can be described as the interference of two conical quasi-Gaussian beams. This is illustrated in Fig.2, which compares the results of numerical simulation of CR intensity distribution in the Lloyd's plane $I = |B_1|^2 + |B_2|^2$ with integrals (1) and with simplified formula (13).
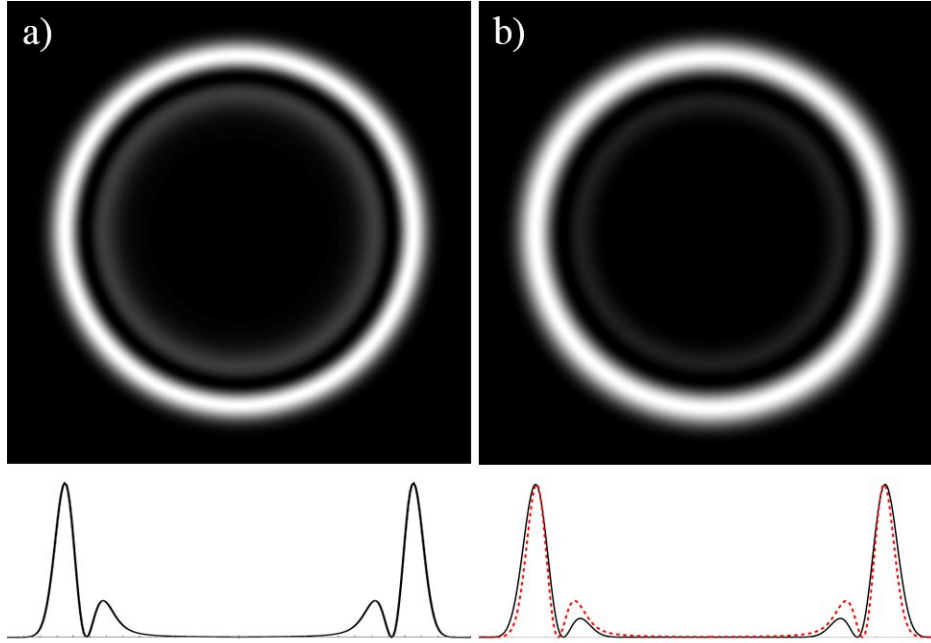

Figure 2. CR intensity distribution in the Lloyd's plane (a) $I = |B_1|^2 + |B_1|^2$ calculated with integrals (1) and (b) calculated with simplified formula (13). The profile of the radial distribution of the CR intensity is shown below. The dotted line shows the radial distribution (a) for comparison.

The suggested simplified quasi-Gaussian solution also predicts the focusing of conically refracted radiation into the Raman spots. However, in the near-axis area the beams undergo self-interference, the consideration of which, as well as a more detailed description of CR phenomenon, we leave for later research.

2.4 Introduction of the M^2 parameter

The full description of the semiconductor laser radiation requires introduction of the beam propagation parameter[16,17] (often termed as the M^2 parameter). As we have approximated the CR field amplitudes as the conical quasi-Gaussian beams, let us substitute, according to the M^2 definition[16] $W \to M^2 W$ and $Z_0 \to M^2 Z_0$. So the intensity distribution in the Lloyd's plane (13) transforms to:

$$I_{M^2}(R,0) = \frac{4A^2 w}{R} \exp\left(-\frac{(R-R_0)^2}{M^2 m^2 w^2}\right) \cos^2\left(\frac{(R-R_0)}{w\sqrt{2}} - \frac{\pi}{4}\right) \tag{14}$$

Comparing (13) and (14) one can notice that the introduction of the beam propagation parameter widens the area of the interference the cones C_1 and C_2 in the Lloyd's plane, which is proportional to the M^2 value. On the other hand, the period of the interference fringes does not depend on the M^2 parameter. Therefore, with $M^2 > 1$ one should observe more than one dark ring in the Lloyd's plane. The results of numerical simulations with (14) for $M^2 = 3$ and $M^2 = 5$ are shown in Fig.3, where one can clearly see 3 and 5 dark rings, correspondingly.
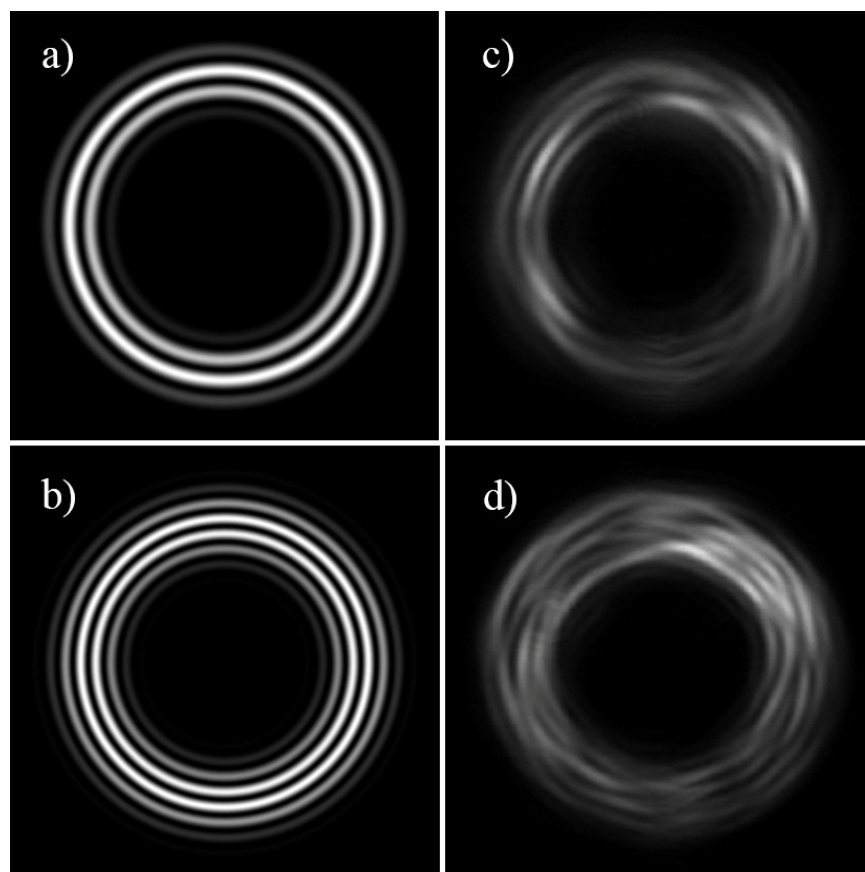
Figure 3. Numerical simulation of intensity distribution of CR radiation of semiconductor laser with $M^2=3$ and $M^2=5$ in the Lloyd's plane (a, b) and results of corresponding experimental measurements (c, d).

3. EXPERIMENT

The schematic view of the setup used in our experiments is shown in Fig. 4. The radiation of the fiber-coupled high-M^2 semiconductor laser was apertured with an iris diaphragm enabling adjustment of the M^2 value.
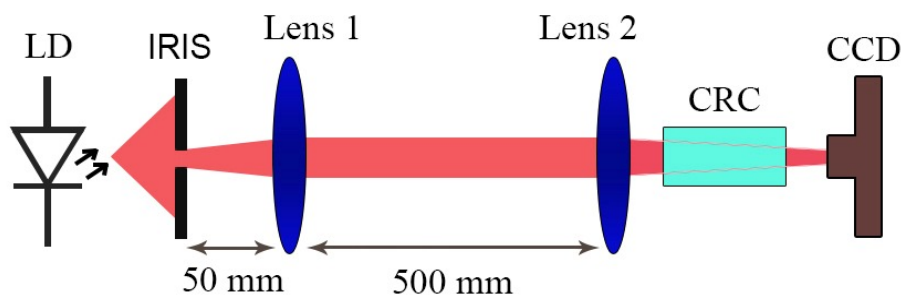

Figure 4. Schematic view of the optical setup used for CR experiments with high-M^2 laser diode (LD). LD radiation passes through the iris diaphragm, collimated with a Lens 1 (focal length 50 mm) and then focused by a Lens 2 (focal length 100 mm) through a conical refraction crystal (CRC). CCD camera detecting an output pattern was mounted on a long-range translation stage enabling registration of the spatial evolution of the conically refracted LD radiation.

The M^2-adjusted laser radiation was collimated using a Lens 1 with 50 mm focal length. The collimated laser beam was then focused by a Lens 2 with 100 mm focal length through a 18-mm long KGW crystal cut along the optical axis. The

value of the beam propagation parameter was measured with a DataRay laser beam analyzer (not shown in the figure) installed between the Lens 1 and Lens 2. The output signal of the CR was detected with a CCD camera mounted on a high-precision translation stage. This enabled observation of the predicted multi-ring CR intensity distributions in the Lloyd's plane. Fig. 3 shows the Lloyd's distributions for $M^2=3$ (Fig.3c) and $M^2=5$ (Fig.3d) with three and five dark rings correspondingly.

4. CONCLUSION

To summarize, the experiments on CR of semiconductor laser radiation with high values of the beam propagation parameter M^2 were performed. CR of laser beams with $M^2=3$ и $M^2=5$ produced unusual Lloyd's intensity distributions with three and five dark rings correspondingly. For interpretation of these observations, a dual-cone model of CR was utilized. The CR cones were represented as the conical quasi-Gaussian beams with the M^2 parameter value of the initial quasi-Gaussian laser beam. This representation enabled clear demonstration of widening of the cones interference area with increase of the M^2 value. On the other hand, the period of interference fringes does not depend on the M^2 parameter. Therefore, the number of dark rings in the Lloyd's distribution appears to be proportional to the M^2 value.

REFERENCES

[1] Hamilton, W. R., "Third supplement to an essay on the theory of systems of rays," Trans. R. Irish Acad. 17, 1-144 (1833).
[2] Lloyd, H., "On the phenomena presented by light in its passage along the axes of biaxial crystals," Phil. Mag. 1, 112-120 and 207-210 (1833).
[3] Poggendorff, J. C., "Ueber die konische Refraction," Annalen der Physic und Chemie, Herausgegeben zu Berlin 48, 461-462 (1839).
[4] Raman, C. V., Rajagopalan, V. S., Nedungadi, T. M. K., "The phenomena of conical refraction," Nature 147, 268 (1941).
[5] Abdolvand, A., Wilcox, K. G., Kalkandjiev, T. K. and Rafailov, E. U. "Conical refraction Nd:KGd(WO$_4$)$_2$ laser," Opt. Express 18, 2753-2759 (2010).
[6] Wilcox, K. G., Abdolvand, A., Kalkandjiev, T. K. and Rafailov, E. U., "Laser with simultaneous Gaussian and conical refraction outputs," App. Phys. B 99, 619-622 (2010).
[7] Loiko, Yu. V., Sokolovskii, G. S., Carnegie, D. J., Turpin, A., Mompart, J., Rafailov, E.U., "Laser beams with conical refraction patterns," Proc. SPIE 8960, 896061 (2014).
[8] McDougall, C., Henderson, R., Carnegie, D. J., Sokolovskii, G. S., Rafailov, E. U., McGloin, D., "Flexible particle manipulation techniques with conical refraction-based optical tweezers," Proc. SPIE 8458, 845824 (2012).
[9] O'Dwyer, D. P., Phelan, C. F., Rakovich, Y. P., Eastham, P. R., Lunney, J. G. and Donegan, J. F., "Generation of continuously tunable fractional optical orbital angular momentum using internal conical diffraction," Opt. Express 18, 16480-16485 (2010).
[10] Rosen, S., Sirat, G. Y., Ilan, H., Agranat, A. J., "A sub wavelength localization scheme in optical imaging using conical diffraction," Opt. Express 21(8), 10133-10138 (2013).
[11] Belskii, M. and Khapaluyk, A. P., "Internal conical refraction of bounded light beams in biaxial crystals," Opt. Spectrosc. 44, 312 (1978).
[12] Berry, M. V., "Conical diffraction asymptotics: fine structure of Poggendorff rings and axial spike," J. Opt. A, Pure Appl. Opt. 6, 289-300 (2004).
[13] Sokolovskii, G. S., Carnegie, D. J., Kalkandjiev, T. K. and Rafailov E. U., "Conical Refraction: New observations and a dual cone model," Opt. Express 21(9), 11125-11131 (2013).
[14] Turpin, A., Loiko, Yu., Kalkandjiev, T.K., Tomizawa, H. and Mompart, J., "On the dual-cone nature of the conical refraction phenomenon," Opt. Lett. 40(8), 1639-1642 (2015).
[15] Gerrard, A. and Burch, J. M., "Introduction to Matrix Methods in Optics", John Wiley & Sons, 116 (1975).
[16] Siegman, A.E., "How to (maybe) measure laser beam quality", OSA Trends in Optics and Photonics Series 17th OSA Annual Meeting (1998).
[17] ISO Standard 11146, "Lasers and laser-related equipment – Test methods for laser beam widths, divergence angles and beam propagation ratios" (2005).